Concurrent Efficient Evaluation of Small-Change Parameters and Green's Functions for TCAD Device Noise and Variability Analysis

Concurrent efficient evaluation of small-change parameters and Green's functions for TCAD device noise and variability analysis

Simona Donati Guerrieri, *Member, IEEE*, Marco Pirola, *Member, IEEE*, Fabrizio Bonani, *Senior Member, IEEE*

***Abstract*—We present here an efficient numerical approach for the concurrent evaluation of the small-change deterministic device parameters and of the relevant Green's functions exploited in the simulation of device small-signal, small-signal large-signal (conversion matrix), stationary and cyclostationary noise, and variability properties of semiconductor devices through the solution of physics-based models based on a partial-differential equation description of charged carrier transport. The proposed technique guarantees a significant advantage in computation time with respect to the currently implemented solutions. The accuracy is the same as for the standard technique.**

***Index Terms*—Numerical simulations, semiconductor device modeling, small-signal parameters, conversion matrix, noise, variability**

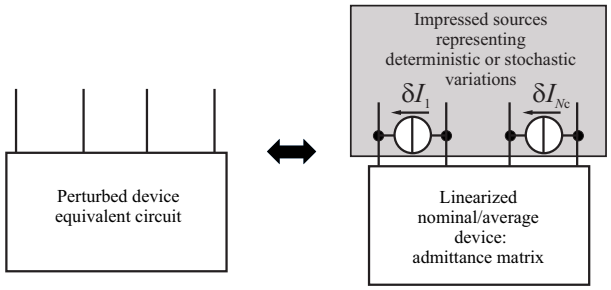

Fig. 1. Linearized representation of a perturbed device including noise/variation equivalent short-circuit current generators (N/VGs). N_c represents the number of device electrical contacts.

I. Introduction

Technology computer-aided design (TCAD) device analysis is increasingly facing the need to cope with the stochastic variations taking place in nanometer scale electron devices. Starting from the well known problem of device electronic noise, the terminal effect of the random fluctuations of microscopic variables taking place in the device volume, TCAD analysis has been recently complemented with an increasing amount of variations, collectively called device *variability analysis*. Variability addresses a wide range of deterministic or random uncertainties such as geometric variations (e.g. gate length uncertainties and line edge roughness), trap and/or doping fluctuations, workfunction spreading etc [1]. Despite noise and variability analyses appear rather different one from the other, they share the need of finding the perturbation of an electrical variable on a device contact (e.g. the electrical current flowing through it) as the result of the variation of physical parameters that takes place in a distributed way inside the device volume. Ultimately, the very difference between noise and variability analysis is the fact that while noise analysis is inherently frequency dependent (noise fluctuations are described by colored stochastic processes, depending on the particular noise process considered), variability is instead dealing with variations that are inherently static. In fact, a unified framework can be devised to treat small device fluctuations within *a linearization of the device response*.

The linearized device is fully represented in terms of a perturbed small-change equivalent circuit, as in the short-circuit representation[1] in Fig. 1, made of two sections: (a) the deterministic (nominal/average) section where the small-change admittance matrix represents the linearized device response in the absence of any fluctuation; and (b) the additional impressed short-circuit current generators, representing the current fluctuations induced by the internal noise or parametric variations. In case of random variations, the average value of the noise/variation generators (N/VGs) is zero and their characterization is made through their statistical second order correlation matrix [2]. The equivalent representation of Fig. 1 is extremely general: for a device linearized around a static (DC) working point, the admittance in Fig. 1 is the *small-signal* (SS) *admittance* matrix which, as the N/VGs, is frequency dependent; if the working point is instead periodic or quasi periodic, the admittance is the so called sideband *conversion matrix* (CM) and the impressed generators are represented in terms of *sideband generators* as a function of the sideband frequency, characterized by the so called *sideband correlation matrix* (SCM) [3].

The deterministic section and the N/VGs of the perturbed equivalent circuit can be determined separately, since they are based on a linearization of the device model. However, the separate knowledge of the two sections is of little practical relevance. The concurrent need of the two parts is especially evident in the most significant published examples of variability of individual cells/circuits studied through TCAD device simulation, e.g. in the variability analysis of a SRAM cell including up to 10 FinFETs [4], or of a large-signal power amplifier [5], [6]. Even in the simple case of stationary noise

The authors are with the Dipartimento di Elettronica e Telecomunicazioni, Politecnico di Torino, Corso Duca degli Abruzzi 24, 10129 Torino, Italy (corresponding author: Simona Donati Guerrieri, e-mail: simona.donati@polito.it).

[1]Clearly several representations are possible in terms of the admittance, impedance or hybrid small-change matrices, any representation being equivalent to the others, at least for well behaved devices.

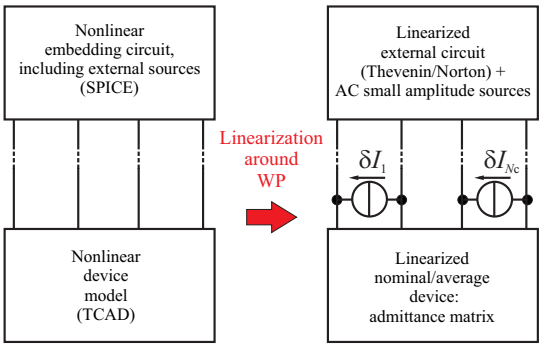

Fig. 2. Schematic representation of a mixed-mode simulation. Left: nonlinear analysis used for the extraction of the device working point (WP). Right: circuit linearized around the WP, including the perturbed linearized device model.

analysis, the knowledge of both the small-signal admittance and of the noise correlation matrix is required, e.g. to calculate the noise figure of a cascaded stage of individual devices using the well-known Friis formula.

From the TCAD standpoint, the two sections of the perturbed device equivalent circuit are usually computed independently: the standard AC analysis [7] is used to extract the deterministic part, while the so-called Green's function (GF) approach [2], [3], [8] is mostly used to characterize the N/VGs. The amount of time required for the two analyses turns out to be comparable, see Sect. II for details.

In this paper, instead, we introduce a general framework for the concurrent evaluation of the small-change admittance matrix and of the N/VGs in both cases of DC and periodic large-signal (LS) device operation. The proposed approach (detailed in Sect. III) essentially extends the GF analysis to include the calculation of the admittance matrix, with negligible computational overhead with respect to the original GF approach [3], [8], yielding a computational advantage of about 50% of the time required for the two separate analyses.

II. Concurrent TCAD evaluation of the small-change parameters and of the N/VGs

In this section we briefly review the standard TCAD procedure for the separate extraction of the admittance matrix and of the N/VGs, and we introduce the main concepts for their concurrent evaluation.

A. Working point determination

The first step in any small-change analysis is the determination of the device working point (WP). As shown in Fig. 2 (left), a mixed-mode TCAD simulation is carried out, where the device physical model is solved with boundary conditions set by the external embedding circuit. In the simplest case the embedding circuit consists of ideal voltage or current generators only, which can be either DC (leading to a static WP) or dynamic (e.g. periodic, leading to a periodic LS WP).

In a more general case, the external circuit contains, besides the generators, linear or nonlinear elements described by compact (SPICE) models. Both the physical model and the external circuit are then linearized (Fig. 2, right) around the WP, to yield an equivalent circuit for the variations. Small variations can be added to the linearized model, including the N/VGs and small-signal AC excitations (if any). The device is now described by the same linearized model of Fig. 1, where each block is evaluated separately by TCAD analysis.

B. Deterministic admittance extraction

The device admittance matrix is usually evaluated by solving the linearized equations of the physical model with proper boundary conditions. To fix the ideas, let us focus on the SS case, i.e. when the WP is static. For the short circuit representation, a unit AC voltage is applied at the angular frequency ω on each of the N_c contacts, while the other contacts are short-circuited [7]. The physical equations are then solved to find the internal solution resulting in the AC currents at all the electrodes. These currents form one row of the small-signal admittance matrix. The required number of solutions of the linearized model is N_c for each frequency. If the WP is periodic, the general picture is the same, but the unit amplitude voltage must be applied at each sideband of the WP harmonics (see Appendix A), yielding the admittance conversion matrix: this small-change description is often called small-signal large-signal (SSLS) analysis. In this case the number of solutions needed is $N_c \times (2N_S + 1)$, for each sideband frequency ω, where N_S is the number of sidebands.

C. Green's function evaluation and N/VGs extraction

N/VGs are usually extracted through the Green's function approach: internal fluctuations are converted into external generators by means of proper convolution integrals of the microscopic distributed variations using the GFs as kernels. To compute the GFs (starting again from the SS case) a unit AC source is applied in each of the internal nodes and each of the physical equations, maintaining the external terminals in short-circuit conditions. The physical system is solved for the internal solution and the external short-circuit currents are evaluated, yielding the elements of the discretized GFs. Such a procedure (called the *direct method*) is extremely long from the computational standpoint, requiring one solution of the linearized equation for each node and each physical equation. To circumvent this problem, starting from the original work from [8], the so-called *generalized adjoint approach* (GAA) has been widely adopted. The GAA basically reverses the role of the injection and observation points, i.e. an AC equivalent source is applied to each of the external terminals and the induced variation is computed in each internal node of the device. The number of solutions required for the GF computation is finally reduced to N_c for each frequency, i.e. the same amount required for the extraction of the admittance matrix. The key feature of this method is that, to invert the injection and observation variables, the system of linearized equations must be transposed, hence the name *transposed method* sometimes used as opposed to the direct (not transposed) one.

The extension of the GAA approach to the LS case is again straightforward: both the unit injections and the observed

variations are now at each sideband of the periodic WP. The Green's function are in this case also describing the conversion of the sidebands from the injection point to the observation point, i.e. they are matrix conversion Green's functions (CGFs).

D. Concurrent admittance and Green's function computation

From the previous review, it is straightforward to see that the complete perturbed device representation of Fig. 1 requires to solve the linearized system of equations twice: once in the direct (not transposed) case to extract the SS matrix, and once for the transposed case to extract the GFs. It is apparent that the amount of linear system solutions required for the combined analyses is $2N_\mathrm{c}$ for each frequency in the SS case and $2N_\mathrm{c}\,(2N_\mathrm{S}+1)$ in the SSLS case.

Surprisingly enough, the fact that the admittance matrix can be regarded as a particular form of Green's function, where the unit injection is placed on a contact instead of an internal point, has been given little attention so far, even if it was already established in the pioneering works on noise analysis [9]: for example, as already explained, the element $(\mathbf{Y})_{i,j}$ of the SS $\mathbf{Y}$ matrix is the current induced at terminal i by a unit voltage applied to terminal j. In fact, any terminal representation of the device AC behavior ($\mathbf{Z}$, $\mathbf{Y}$ or hybrid matrix) is inherently a sub-case of the more general variational problem.

It is therefore possible to define an extended Green's function whose value equals the original GF for the internal nodes and the admittance matrix on the contact nodes. In Sec. III we follow such an idea and define the needed model equations. Further, we demonstrate that a straightforward extension of the GAA method [8] allows for its efficient evaluation, requiring the solution of the transposed system only, with a negligible overhead with respect to the original transposed system of [8]. The direct solution can be therefore completely omitted.

III. Model equations and proposed approach

In order to introduce the efficient concurrent computation of the terminal small-change parameters and of the Green's functions, we start from the discretized model equations making use of a notation akin to the one in [3]. For simplicity, we consider here the case of a bipolar drift-diffusion transport model, characterized by the electrostatic potential φ and the electron (n) and hole (p) free carrier concentrations as unknowns. However, the extension to the case on any PDE-based physical model, such as the energy balance transport and/or the inclusion of heat transport, is trivial.

Let us consider a discretization mesh made on N nodes. The total number of contacts is N_c, and we denote as $\mathbf{i}_\mathrm{c}$ (resp., $\mathbf{v}_\mathrm{c}$) the vector representing the set of N_c contact currents (resp., external voltages).

The discretization of the model on the internal nodes leads to the following $3\times N$ equations, deriving from the discretization of the model and including the boundary conditions on the device boundaries ($\alpha=\varphi,n,p$):

$$\mathbf{f}_\alpha\left(\boldsymbol{\varphi},\mathbf{n},\mathbf{p};\dot{\mathbf{n}},\dot{\mathbf{p}}\right)=\mathbf{0}\qquad \mathbf{b}_\alpha\left(\boldsymbol{\varphi},\mathbf{n},\mathbf{p};\dot{\mathbf{n}},\dot{\mathbf{p}},\mathbf{v}_\mathrm{c}\right)=\mathbf{0}, \tag{1a}$$

where $\dot{x}=\mathrm{d}x/\mathrm{d}t$, and $\mathbf{f}_\varphi$, $\mathbf{f}_n$, $\mathbf{f}_p$ represent, respectively, the discretized Poisson, electron continuity and hole continuity equations in the internal nodes. Finally, $\mathbf{b}_\varphi$, $\mathbf{b}_n$ and $\mathbf{b}_p$ are the corresponding discretized boundary conditions.

The $2N_\mathrm{c}$ equations needed to close the system in the $3N+2N_\mathrm{c}$ unknowns are provided by the constitutive relationships of the external circuit connected to the N_c device terminals:

$$\mathbf{e}\left(\mathbf{v}_\mathrm{c},\mathbf{i}_\mathrm{c};\frac{\mathrm{d}}{\mathrm{d}t}\right)=\mathbf{s}, \tag{1b}$$

where $\mathbf{s}(t)$ is the set of external sources, and by the constitutive equations of the contact currents $\mathbf{i}_\mathrm{c}$ as a function of the nodal unknowns:

$$\mathbf{c}\left(\boldsymbol{\varphi},\mathbf{n},\mathbf{p},\mathbf{i}_\mathrm{c};\dot{\mathbf{n}},\dot{\mathbf{p}}\right)=\mathbf{0}. \tag{1c}$$

Solving system (1) corresponds to find the WP. The system is then linearized around the WP, and the circuit equations (1b) are substituted by properly dedicated boundary conditions (e.g. short-circuit): in the following Sec.III-A we first consider the static WP case (SS analysis), to extend it to the periodic WP case in Sec. III-B, with the aid of the formulation provided in Appendix A.

A. Green's function approach to SS AC analysis

The model (1) is linearized around the DC working point and the analysis is carried out in the frequency domain [7] where all the variables are represented by their complex phasors, hereafter denoted by a tilde on the variable. Turning off at first all excitations ($\delta\tilde{\mathbf{v}}_\mathrm{c}=\mathbf{0}$, i.e. enforcing short-circuit conditions), we define the homogeneous system

$$\begin{bmatrix}\tilde{\mathbf{J}}_\mathrm{ph} & \tilde{\mathbf{J}}_\mathrm{Bv} & \mathbf{0}\\ \mathbf{0} & \mathbf{I}_{N_\mathrm{c}} & \mathbf{0}\\ \tilde{\mathbf{J}}_\mathrm{c}^\mathrm{T} & \mathbf{0} & -\mathbf{I}_{N_\mathrm{c}}\end{bmatrix}\begin{bmatrix}\delta\tilde{\mathbf{x}}\\ \delta\tilde{\mathbf{v}}_\mathrm{c}\\ \delta\tilde{\mathbf{i}}_\mathrm{c}\end{bmatrix}=\begin{bmatrix}\mathbf{0}\\ \mathbf{0}\\ \mathbf{0}\end{bmatrix} \tag{2}$$

where $\tilde{\mathbf{J}}_\mathrm{ph}$ and $\tilde{\mathbf{J}}_\mathrm{Bv}$ are matrices collecting the Jacobian of the discretized equations (1a) and have dimensions $3N\times 3N$ and $3N\times N_\mathrm{c}$, respectively. $\mathbf{I}_{N_\mathrm{c}}$ is the identity matrix of size $N_\mathrm{c}\times N_\mathrm{c}$, while $\delta\tilde{\mathbf{x}}$ represents the collection of the nodal values of the microscopic variables $\delta\varphi,\delta n,\delta p$. Finally $\tilde{\mathbf{J}}_\mathrm{c}^\mathrm{T}$ is a complex matrix related to the Jacobian of (1c) with dimension $N_\mathrm{c}\times 3N$.

To define the extended GFs, a unit impulsive source term is placed sequentially in each of the mesh nodes, i.e. at the right hand side of the first N equations of (2) and, again sequentially, on each device contacts, i.e. at the right-hand side of the second equation block of (2):

$$\begin{bmatrix}\tilde{\mathbf{J}}_\mathrm{ph} & \tilde{\mathbf{J}}_\mathrm{Bv} & \mathbf{0}\\ \mathbf{0} & \mathbf{I}_{N_\mathrm{c}} & \mathbf{0}\\ \tilde{\mathbf{J}}_\mathrm{c}^\mathrm{T} & \mathbf{0} & -\mathbf{I}_{N_\mathrm{c}}\end{bmatrix}\begin{bmatrix}\delta\tilde{\mathbf{x}}\\ \delta\tilde{\mathbf{v}}_\mathrm{c}\\ \delta\tilde{\mathbf{i}}_\mathrm{c}\end{bmatrix}=\begin{bmatrix}\mathbf{S}_\mathrm{ph} & \mathbf{0}\\ \mathbf{0} & \mathbf{S}_\mathrm{c}\\ \mathbf{0} & \mathbf{0}\end{bmatrix} \tag{3}$$

where $\mathbf{S}_\mathrm{ph}$ is a $3N\times 3N$ diagonal matrix with unit entries; $\mathbf{S}_\mathrm{c}$ is instead a (unit) diagonal $N_\mathrm{c}\times N_\mathrm{c}$ matrix, representing injections of unit voltages on the device terminals. The system with such injection matrices must be solved to compute $\delta\tilde{\mathbf{i}}_\mathrm{c}$: if the injection is on the internal nodes, then $\delta\tilde{\mathbf{v}}_\mathrm{c}=\mathbf{0}$ effectively ensures that these currents are evaluated in short circuit conditions; if the injection is on contact j, then the

currents are evaluated in short circuit conditions apart for terminal j, hence the N_c currents found represent the j-th row of the admittance matrix. The direct solution of (3) requires $3N+N_c$ back-substitutions: to avoid this, we extend the GAA method of [8]. Defining

$$\tilde{\mathbf{J}} = \begin{bmatrix} \mathbf{J}_{ph} & \mathbf{J}_{Bv} \\ \mathbf{0} & \mathbf{I}_{N_c} \end{bmatrix} \qquad \delta\tilde{\mathbf{z}} = \begin{bmatrix} \delta\tilde{\mathbf{x}} \\ \delta\tilde{\mathbf{v}}_c \end{bmatrix} \qquad \mathbf{S} = \begin{bmatrix} \mathbf{S}_{ph} & \mathbf{0} \\ \mathbf{0} & \mathbf{S}_c \end{bmatrix} \tag{4}$$

and $\tilde{\mathbf{A}}^T = [\tilde{\mathbf{J}}_c^T, \mathbf{0}]$, equation (3) takes the form

$$\begin{bmatrix} \tilde{\mathbf{J}} & \mathbf{0} \\ \tilde{\mathbf{A}}^T & -\mathbf{I}_{N_c} \end{bmatrix} \begin{bmatrix} \delta\tilde{\mathbf{z}} \\ \delta\tilde{\mathbf{i}}_c \end{bmatrix} = \begin{bmatrix} \mathbf{S} \\ \mathbf{0} \end{bmatrix}. \tag{5}$$

A simple analysis [8] of (5) based on the formal solution of the first $3N + N_c$ equations:

$$\delta\tilde{\mathbf{z}} = \tilde{\mathbf{J}}^{-1}\mathbf{S} \tag{6}$$

substituted in the last N_c equations:

$$\delta\tilde{\mathbf{i}}_c = \tilde{\mathbf{A}}^T\tilde{\mathbf{J}}^{-1}\mathbf{S} = \tilde{\mathbf{y}}^T\mathbf{S} \tag{7}$$

suggests the adoption of the following generalized adjoint approach. First, matrix $\tilde{\mathbf{y}}$ (size $(3N + N_c) \times N_c$) is computed solving N_c times the transposed linear system (size $(3N + N_c) \times (3N + N_c)$)

$$\tilde{\mathbf{J}}^T\tilde{\mathbf{y}} = \tilde{\mathbf{A}} \tag{8}$$

and finally the short circuit terminal current variations $\delta\tilde{\mathbf{i}}_c$ are found by means of the matrix product

$$\delta\tilde{\mathbf{i}}_c = \tilde{\mathbf{y}}^T\mathbf{S} \tag{9}$$

that requires a negligible computation time.

Notice that due to the structure of $\mathbf{S}$, the first $3N$ rows of $\tilde{\mathbf{y}}$ correspond to the injection into the mesh nodes, and therefore to the conventional GFs, while the last N_c rows of $\tilde{\mathbf{y}}$ are the response to the injection in the terminal voltages, and thus correspond to the device SS $\mathbf{Y}$ matrix. Hence the vector $\tilde{\mathbf{y}}$ effectively represents the extended GF.

B. Green's function approach to LS SSLS analysis

Let us consider any discretized variable $\boldsymbol{\alpha}(t)$. Its perturbation around the LS working point is denoted, in time domain, as $\delta\boldsymbol{\alpha}(t)$ and, according to [3], it can be expressed as a superposition of frequency sidebands as the real part of a complex signal characterized by $2N_S + 1$ (upper) sideband (absolute) angular frequencies $\omega_k^+ = \omega_k + \omega$, and an equal number of sideband harmonic amplitudes (see Appendix A for details).

Concerning the jacobian matrices required for the extension of (3), the same formulation valid for the SS analysis actually holds, where however each matrix element is substituted by a $(2N_S + 1) \times (2N_S + 1)$ CM built according to the frequency domain representation of the time derivative operator (for the memory part) and to the Toeplitz matrix expansion (for the instantaneous part) as discussed in Appendix A, yielding a system of the total dimension of $[(3N + 2N_c)(2N_S + 1)] \times [(3N + 2N_c)(2N_S + 1)]$. Once the extended system is defined, following the same steps of the GAA method (from (3) to (9)) the device admittance CM and the CGFs can be concurrently evaluated by means of $N_c(2N_S+1)$ solutions of the transposed linear system, thus gaining a huge computational advantage with respect to the direct computation.

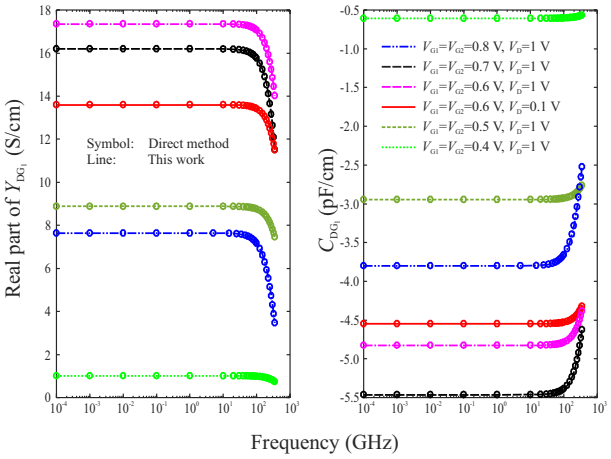

Fig. 3. Real and Imaginary (divided by the angular frequency) part of Drain-Gate1 element of the SS admittance matrix of the double gate device (Gate1 is one of the two gates).

IV. Results

To validate the approach, we show here selected results showing that the proposed extended GAA method yields the SS and SSLS admittance matrices identical to the ones obtained with the direct method. GF functions are not reported since they are by definition identical to the original approach [2], [3], [8]. All results have been obtained with an in-house 2D simulator implementing the bipolar drift-diffusion model and exploiting the harmonic balance method for periodic LS simulations.

As a first case we consider the SS admittance matrix of a double gate 54 nm gate length Si FinFET device (the structure shown in [10]), with 1 nm equivalent gate oxide, Si fin (10 nm width and 10^{15} cm^{-3} bulk acceptor doping) and source/drain extensions of 54 nm length and 5×10^{18} cm^{-3} donor doping. Figs. 3-6 show the real and imaginary parts of the elements of the admittance matrix at various bias points as a function of frequency. Symbols are obtained with the direct method, lines with the new approach: the two procedures yield identical results.

As the second case study we consider a GaAs microwave MESFET with a uniformly doped ($N_D = 2 \times 10^{17}$ cm^{-3}) channel layer with 0.17 μm thickness, 0.5 μm gate contact length and 5 eV gate workfunction. The contact separation is 0.5 μm. The gate width is normalized to 1 mm. The device is included in a class A power amplifier circuit (see [6] for details) with a tuned load (i.e., the current higher harmonics are short-circuited), operating at the nominal frequency of 10 GHz. The class A bias point is $V_{GS} = -1.5$ V and $V_{DS} = 9$ V. The SSLS admittance conversion matrix has been evaluated at the input power of 23.1 dBm, close to the 1 dB compression point of the amplifier. Figs. 7 and 8 show some elements of the Drain-Gate and Gate-Gate components of the admittance CM:

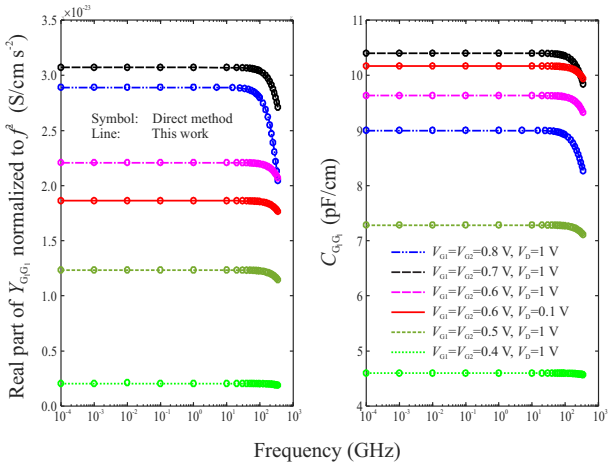

Fig. 4. Real and Imaginary part (divided by the angular frequency) of Gate1-Gate1 element of the SS admittance matrix of the double gate device (Gate1 is one of the two gates).

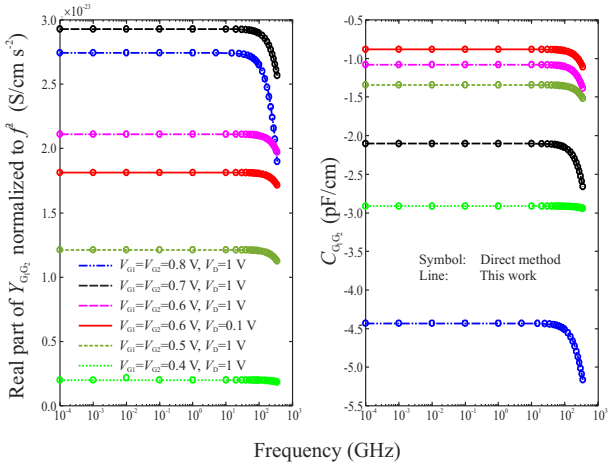

Fig. 5. Real and Imaginary part (divided by the angular frequency) of Gate1-Gate2 element of the SS admittance matrix of the double gate device (Gate1 and Gate2 are the two gates).

the diagonal terms represent the correlation between the same sideband, while the off-diagonal terms are related to frequency conversion between different sidebands: again the agreement is perfect.

V. Conclusions

We have demonstrated an extension of the numerical approach originally devised for the efficient computation of the Green's functions exploited in noise and variability device TCAD simulations that permits the concurrent evaluation of the small-change deterministic device parameters and of the GFs yielding the noise/variability equivalent device generators. The extended method has a negligible impact on both the linear system assembly and on the corresponding solution, and guarantees an advantage of about 50% in computation time with respect to the standard, separate evaluations.

Furthermore, by comparing the direct and proposed approaches to two relevant simulation case studies (a Si double gate FinFET, and a mixed mode simulation of a GaAs MESFET based power amplifier) we also show no difference in the simulation results and accuracy.

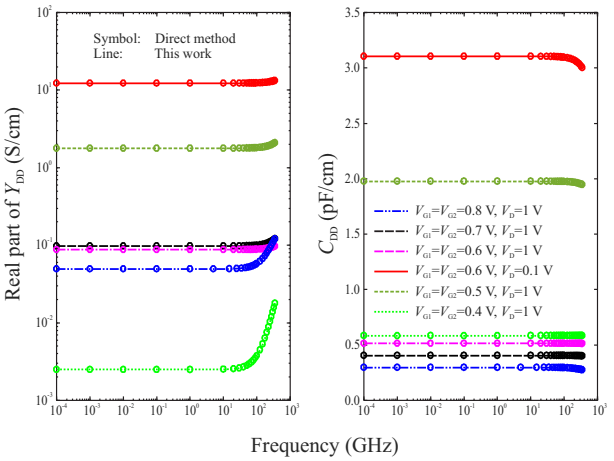

Fig. 6. Real and Imaginary part of Drain-Drain element of the SS admittance matrix of the double gate device.

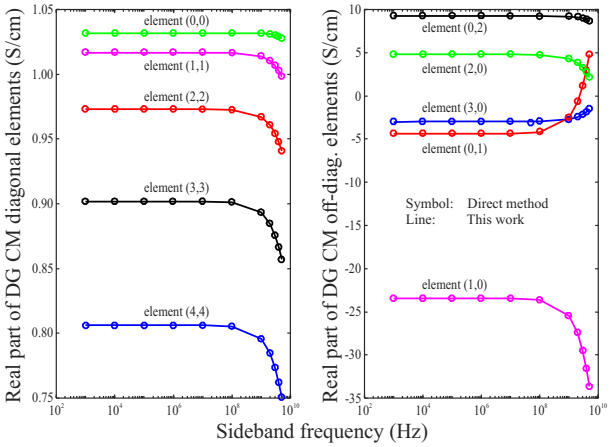

Fig. 7. Real part of Drain-Gate element of the SSLS admittance conversion matrix of the MESFET device. Left: diagonal terms; right: off-diagonal terms.

Appendix A
Frequency domain LS and SSLS formalism

This Appendix is devoted to a brief review of the frequency domain formalism used in the paper. The contents are mostly adapted from [2], [3].

We treat here a scalar nonlinear system to keep the notation simple. The extension to the vector case is obvious, although formally involved. Let us consider the nonlinear forced equation

$$\dot{x} + f(x) = s(t) \tag{10}$$

where $s(t)$ is a periodic function of time of period T. Because of time periodicity, both $x(t)$ and $s(t)$ can be expanded in Fourier series[2]

$$x(t) = \sum_k \tilde{x}_k \, \mathrm{e}^{\mathrm{j}\omega_k t} \tag{11}$$

[2]The case of quasi-periodic, i.e. multi-tone, excitation can be treated similarly, exploiting a multi-dimensional index for the Fourier representation.

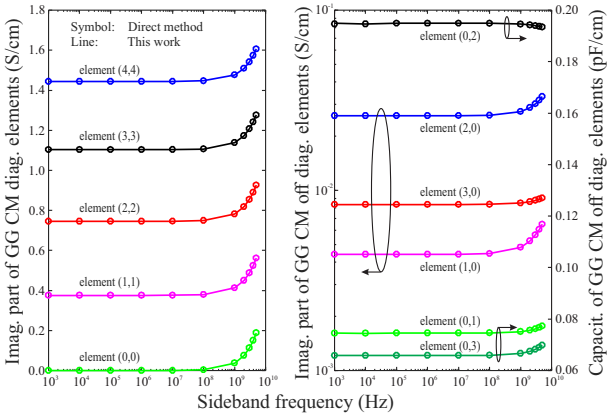

Fig. 8. Imaginary part of Gate-Gate element of the SSLS admittance conversion matrix of the MESFET device. Left: diagonal terms; right: off-diagonal terms (absolute values). Some off-diagonal elements have been normalized by the angular frequency (capacitance) for better representation.

where $\omega_k = k\omega_0$ is the (angular) frequency of the k-th harmonic of $x(t)$, $\omega_0 = 1/T$, and $\tilde{x}_k$ is the k-th harmonic (complex) amplitude. The summation index k, mathematically running on all the integers with sign, is in practice limited to a maximum number of harmonics N_L, so that $k = -N_\mathrm{L}, \ldots, 0, \ldots, N_\mathrm{L}$. For the sake of simplicity, we consider here the exponential form of the Fourier representation that, for real signals, is characterized by the condition

$$\tilde{x}_{-k} = \tilde{x}_k^* \tag{12}$$

where * denotes complex conjugation. In other words, (11) is fully identified by $2N_\mathrm{L}+1$ real numbers, allowing for the reconstruction of the entire set of harmonic amplitudes. Substituting (11) into (10), the differential equation is converted into an algebraic equation system having as unknowns the harmonic amplitudes $\tilde{\mathbf{x}} = [\tilde{x}_{-N_\mathrm{L}}, \ldots, \tilde{x}_{N_\mathrm{L}}]^\mathrm{T}$ ($^\mathrm{T}$ denotes the transpose), leading to the so called Harmonic Balance (HB) formulation [11].

The definition of the Small-Signal Large-Signal (conversion) analysis requires to study a perturbation of (10) around its steady-state solution, represented by the set of harmonic amplitudes that satisfy the HB algebraic system. A trivial linearization of (10) leads to

$$\delta\dot{x} + g(t)\delta x(t) = \delta s(t) \tag{13}$$

where $\delta x(t)$ is the perturbation of the solution with respect to the steady state , $g(t)$ is a T-periodic function being the derivative of $f(t)$ calculated in the periodic working point, and $\delta s(t)$ is a properly chosen source term. According to the SS-LS theory, the relevant signals $\delta x(t)$ and $\delta s(t)$ can be expressed in the frequency domain (double-sided spectrum) as

$$\delta x(t) = \Re\left\{\sum_k \delta\tilde{x}_k^+ \, \mathrm{e}^{\mathrm{j}\omega_k^+ t}\right\}. \tag{14}$$

where $\omega_k^+ = \omega_k + \omega$ are the so-called *sidebands* (ω is the sideband frequency) and $\delta\tilde{x}_k^+$ complex coefficients. Notice that the k index, in principle running on all integers (with sign), is in practice limited to a finite value N_S, linked to the number of harmonics of the LS steady state, i.e. $N_\mathrm{L} = 2N_\mathrm{S}$ [3].

Substituting the Fourier expansion of $g(t)$ and the sideband harmonic representations of $\delta x(t)$ and $\delta s(t)$ into (13), the upper sideband amplitudes are found to satisfy

$$\mathrm{j}\omega_k^+\delta\tilde{x}_k^+ + \sum_n \tilde{g}_{k-n}\delta\tilde{x}_n^+ = \delta\tilde{s}_k^+. \tag{15}$$

Equation (15) admits of a matrix representation, defining the corresponding conversion matrix.

$$\mathbf{\Omega}^+\delta\tilde{\mathbf{x}}^+ + \mathbf{T}_g\delta\tilde{\mathbf{x}}^+ = \delta\tilde{\mathbf{s}}^+ \tag{16}$$

where $\mathbf{\Omega}^+$ (size $(2N_\mathrm{S}+1)\times(2N_\mathrm{S}+1)$) represents the time derivative operator (diagonal matrix in the exponential form of the Fourier series), and $\mathbf{T}_g$ (size $(2N_\mathrm{S}+1)\times(2N_\mathrm{S}+1)$) is the Toeplitz matrix built starting from the harmonic amplitudes of $g(t)$. The (m,n) element of $\mathbf{T}_g$ is given by

$$(\mathbf{T}_g)_{m,n} = \tilde{g}_{m-n}. \tag{17}$$

Inverting (16) we find

$$\delta\tilde{\mathbf{x}}^+ = \mathbf{C}(\omega)\delta\tilde{\mathbf{s}}^+; \quad \mathbf{C}(\omega) = (\mathbf{\Omega}^+ + \mathbf{T}_g)^{-1} \tag{18}$$

where $\mathbf{C}$ is the conversion matrix (CM) associated to linear system (13). Finally, this formalism can be extended to the vector case assuming that variables $x(t)$, $s(t)$ and $g(t)$ become size N vectors, and in (18) $\delta\tilde{\mathbf{x}}^+$ and $\delta\tilde{\mathbf{s}}^+$ are $[(2N_\mathrm{S}+1)N]\times(2N_\mathrm{S}+1)$ matrices, and $\mathbf{C}$ is a $[(2N_\mathrm{S}+1)N]\times[(2N_\mathrm{S}+1)N]$ matrix.

References

[1] A. Asenov, A. Brown, J. Davies, S. Kaya, and G. Slavcheva, "Simulation of intrinsic parameter fluctuations in decananometer and nanometer-scale MOSFETs," *IEEE Trans. El. Dev.*, vol. 50, no. 9, pp. 1837–1852, September 2003.

[2] F. Bonani and G. Ghione, *Noise in semiconductor devices*. Heidelberg: Springer-Verlag, 2001.

[3] F. Bonani, S. Donati Guerrieri, G. Ghione, and M. Pirola, "A TCAD approach to the physics-based modeling of frequency conversion and noise in semiconductor devices under large-signal forced operation," *IEEE Trans. El. Dev.*, vol. 48, no. 5, pp. 966–977, May 2001.

[4] Modeling statistical variability of static noise margins of SRAM cells using the statistical impedance field method, TCAD Sentaurus example, version l-2016.03, march 2016. [Online]. Available: http://www.synopsys.com/Tools/silicon/tcad/device-simulation/Pages/sentaurus-device.aspx

[5] S. Donati Guerrieri, F. Bonani, and G. Ghione, "A novel approach to microwave circuit large-signal variability analysis through efficient device sensitivity-based physical modeling," in *International Microwave Symposium*, San Francisco (CA), 2016.

[6] S. Donati Guerrieri, F. Bonani, F. Bertazzi, and G. Ghione, "A unified approach to the sensitivity and variability physics-based modeling of semiconductor devices operated in dynamic conditions. Part I: Large-signal sensitivity," *IEEE Trans. El. Dev.*, vol. 63, no. 3, pp. 1195–1201, March 2016.

[7] S. Laux, "Techniques for small-signal analysis of semiconductor devices," *IEEE Trans. Computer-Aided Design Integr. Circuits Syst.*, vol. 4, no. 4, pp. 472–481, 1985.

[8] F. Bonani, G. Ghione, M. Pinto, and R. Smith, "An efficient approach to noise analysis through multidimensional physics-based models," *IEEE Trans. El. Dev.*, vol. 45, no. 1, pp. 261–269, Jan. 1998.

[9] G. Ghione and F. Filicori, "A computationally efficient unified approach to the numerical analysis of the sensitivity and noise of semiconductor devices," *IEEE Trans. Computer-Aided Design Integr. Circuits Syst.*, vol. 12, no. 3, pp. 425–438, 1993.

[10] A. M. Bughio, S. D. Guerrieri, F. Bonani, and G. Ghione, "Physics-based modeling of FinFET RF variability," in *European Microwave Integrated Circuits Conference*, London, UK, 2016.

[11] K. Kundert, A. Sangiovanni-Vincentelli, and J. White, *Steady-state methods for simulating analog and microwave circuits*, K. Kundert, A. Sangiovanni-Vincentelli, and J. White, Eds. Boston: Kluwer Academic Publisher, 1990.